Crystalline structure of TiC ultra thin layers formed on highly oriented pyrolytic graphite by chemical reaction from Ti/graphite system

Osamu Nakatsuka[1,*], Kenji Hisada[1,†], Satoshi Oida[1,‡], Akira Sakai[2], and Shigeaki Zaima[1,3]

[1] *Department of Crystalline Materials Science, Graduate School of Engineering, Nagoya University, Nagoya 464-8603, Japan*
[2] *Graduate School of Engineering Science, Osaka University, Toyonaka, Osaka 560-8531, Japan*
[3] *Institute of Materials and Systems for Sustainability, Nagoya University, Nagoya 464-8603, Japan*

[*]E-mail: nakatuka@alice.xtal.nagoya-u.ac.jp

We have investigated the atomic-scale reaction between a Ti thin layer and highly oriented pyrolytic graphite (HOPG) mainly by scanning tunneling microscopy. A deposited Ti layer shows an epitaxial orientation structure on a HOPG substrate even in room-temperature deposition, while the bonding between Ti and HOPG is very weak. The chemical reaction between Ti and HOPG takes place, and epitaxial TiC domains on HOPG are formed for annealing at above 600 °C. The TiC domains shows a smooth surface corresponding to the TiC(111) plane after annealing at 700 °C. The formation of TiC(001) facets and significant surface roughening of not only TiC but also HOPG substrates are observed for annealing at as high as 900 °C.

† Present address: DENSO Corporation, Nukata-Gun, Aichi 444-0193, Japan
‡ Present address: IBM T. J. Watson Research Center, New York 10598, USA

1. Introduction

Carbon (C)-related low-dimensional structures such as graphene sheets and nanotubes have attracted attention for nanoelectronic applications because of the high mobility of both their electrons and holes and their characteristic electronic properties[1-7]. For the application of low-dimensional C materials in nanoelectronic devices, it is necessary to control the crystalline structure of not only the C material itself but also insulators, metals, and interfaces of device structures on the atomic scale. Also, in the development of device applications of C nanostructures, there are many challenges for metal/semiconductor contact technologies to achieve low contact resistance, high thermal robustness, high adhesive property, and high reliability [8-13].

Understanding the crystalline structure and chemical reaction at the interface between a metal electrode layer and a C nanostructure is essential for attaining high performance and reliability of the contact structure between metal and C-related materials. However, it is difficult to analyze these properties in atomic-scale C nanostructures in detail because of the limitation of the volume of low-dimensional C nanomaterials. On the other hand, highly oriented pyrolytic graphite (HOPG) consists of high-quality stacked graphite monolayers, and thus it is a good specimen for the fundamental study of metal/C nanostructure contact. There are many previous studies of the behavior and crystalline structure of some metals, such as Cu[14,15], Ni[15,16], Pt[15,17], Ag[18,19], and Co[20], deposited on graphite substrates. Also, scanning tunnel microscopy (STM) studies of the nanostructure of metals on graphite substrates have been reported[21-25]. However, these previous studies of the metal/graphite substrate system basically focused on the nanostructures of metals deposited on substrates, and studies focusing on the metal/graphite contact structure and interfacial reaction are limited. The relationship between the crystalline structure and the chemical reaction between a metal and a graphite substrate has not yet been understood in

detail.

In this study, we examined the deposition of multi-monolayers of a titanium (Ti) thin film directly on a HOPG substrate and analyzed the atomic structure of the sample surface by STM and photoelectron spectroscopic techniques to investigate the crystalline structures and chemical reaction of a Ti layer with graphite after annealing.

2. Experimental methods

HOPG was used as the substrate. Its surface was cleaned by peeling the surface graphite layers off with an adhesive tape followed by annealing at 1000 °C in an ultrahigh-vacuum (UHV) chamber whose base pressure was below 3×10^{-8} Pa. The surface of HOPG was confirmed to be clean by in situ reflection high-energy electron diffraction (RHEED) and STM. After cleaning the surface, Ti layers with thicknesses of 0.05–0.25 nm were successively deposited using an electron beam evaporation system at a pressure below 1×10^{-7} Pa at room temperature (RT). Then, Ti/HOPG samples were annealed at temperatures ranging from 600 to 1000 °C at a pressure below 1×10^{-6} Pa in the same UHV chamber.

The crystalline structure and morphology of the sample surface were observed by in situ RHEED and STM. The chemical bonding structure of surface layers in Ti/HOPG samples was analyzed by ex situ X-ray photoelectron spectroscopy (XPS) using a Mg Kα X-ray source (photon energy; $h\nu$ = 1254 eV).

3. Results and discussion

Figures 1(a)-1(d) show STM images of the Ti (thickness: 0.05 nm)/HOPG and Ti

(thickness: 0.25 nm)/HOPG samples. Figures 1(b) and 1(d) are enlarged images of Figs. 1(a) and 1(c), respectively. In the Ti (thickness: 0.05 nm)/HOPG sample, many small particle-like bright spots are observed on the terrace of HOPG in Fig. 1(a). Also, protrusions along the step edge lines can be observed. These small particles and protrusions are considered to be agglomerated structure of deposited Ti. Note that we firstly observed the STM image shown in Fig. 1(b) and then observed the image in Fig. 1(a). After observing the magnified STM image shown in Fig. 1(b), we found that there are no small particles in the region first observed in Fig. 1(a). This result suggests that the Ti particles were swept out and agglomerated at edge lines, and the as-deposited Ti atoms very weakly interacted with the HOPG surface, which is energetically stable.

For the deposited Ti thickness as thick as 0.25 nm, the agglomerated structure shows the characteristic threefold symmetry, as shown in Fig. 1(c). The in situ RHEED pattern obtained from this sample immediately after the Ti deposition is shown in Fig. 2. A streak with a ring pattern is clearly observed. The characteristic distances d_1 and d_2 were estimated to be 0.297±0.004 and 0.513±0.004 nm, respectively, from the diffraction pattern shown in Fig. 2. These values correspond to the lattice planes of hexagonal Ti(1000) (d = 0.296 nm) and Ti(11$\bar{2}$0) (d = 0.513 nm)[26]. These values can be associated with the hexagonal structure of Ti domains and indicate the epitaxial growth of Ti thin layers on HOPG. The epitaxial relationship between Ti and the HOPG substrate can be determined to be Ti(0001)//HOPG(0001) and Ti[11$\bar{2}$0]//HOPG[11$\bar{2}$0] from the RHEED pattern.

We deduced that this characteristic structure is related to the Van der Waals epitaxy[27,28] of a Ti thin layer on the HOPG substrate. Van der Waals epitaxy was also previously reported in the growth of thin films such as GaSe on MoS_2[29] and $CrPt_3$ on WSe_2[30]. It is known that this characteristic growth is observed in the case of thin-film

growth on an energetically inactive surface of a substrate. In addition, the condition of the long-range periodic structure with a large lattice mismatch between the grown film and the substrate is required for this epitaxy. In fact, it is well known that an HOPG surface is relatively energetically stable and the lattice mismatch between Ti and HOPG is as large as 20%, considering the epitaxial relationship mentioned above. This means that the bonding of the Ti layer with the HOPG substrate just by Van der Waals force is very weak, which is consistent with the sweeping out of the agglomerated Ti particles at step edges just by tip scanning in the very thin Ti layer deposited on HOPG, which is observed in the STM image shown in Fig. 1(a).

Next, we examined the in situ annealing of Ti/HOPG samples under UHV condition. Figures 3(a)-3(c) show STM images of Ti (thickness: 0.25 nm)/HOPG samples after in situ annealing at 700, 900, and 1000 °C, respectively. The surface profiles at the position indicated in these images by arrows are also shown below the STM images. After annealing at 700 °C, many hexagonal domains with atomically flat and uniform surfaces are formed on the HOPG terrace. On the other hand, after annealing above 900 °C, the symmetry of the domains significantly degrades as they agglomerate with significant roughening of the domain surface. In addition, after annealing at 1000 °C, significant erosion of the HOPG substrate around the domains is observed as a dip at the edge region of the domains as indicated by red arrows in the surface profile shown in Fig. 3(c).

Figures 4(a)-4(c) show the RHEED patterns of the Ti (thickness: 0.25 nm)/HOPG samples after in situ annealing at 700, 900, and 1000 °C, respectively. After 700 °C annealing in UHV, the characteristic distances d_3 and d_4 shown in Fig. 3(a) were estimated to be 0.306±0.004 and 0.531±0.004 nm, respectively. These values correspond to the lattice planes of Ti carbide, TiC(100) (d = 0.306 nm), and TiC(111) (d = 0.530 nm)[26]. The

STM and RHEED results indicate the epitaxial growth of a TiC layer on HOPG due to the chemical reaction between Ti and HOPG. The epitaxial relationship between TiC and HOPG is determined to be TiC(111)//HOPG(0001) and TiC[$1\bar{1}0$]//HOPG[$11\bar{2}0$]. Moreover, after 900 °C annealing, the streak in the diffraction pattern becomes spotty, indicating the degradation of the TiC layer with the formation of a 3D island-like morphology, which is consistent with the observation from the STM image shown in Fig. 3(b).

Here, we deduce the morphological transition of the TiC layer on HOPG depending on the annealing condition. After annealing below 700 °C, the TiC layer shows a smooth surface corresponding to the TiC(0001) plane (c-plane). Ito et al. previously reported the STM observation of the epitaxial growth of a graphite monolayer on a TiC(111) surface[31]. They found that the graphite monolayer grows showing that the azimuthal relationship with TiC is C[$11\bar{2}0$]//TiC[$1\bar{1}0$], which is consistent with the observed crystalline structure in this study. They note that, with this relationship, one-seventh of the reciprocal space unit vector of TiC[$1\bar{1}0$] corresponds to one-fifteenth of that of the graphite along [$11\bar{2}0$], and one-fourteenth of the reciprocal lattice of TiC[$11\bar{2}$] corresponds to one-tenth of that of graphite along [$10\bar{1}0$]. We deduce that this long-range matching with the superlattice would lead to the formation of a TiC epitaxial layer on HOPG at a temperature of 700 °C.

On the other hand, after annealing above 900 °C, the agglomeration of TiC is observed and the domains show a 3D-like pyramidal shape surrounded by TiC{1000} a-plane facets. This result is taken into account from the viewpoint of the surface energy of TiC. Dudiy et al. reported that the surface energies of TiC(100), TiC(110), and TiC(111) with the relaxed structure are theoretically calculated 1.73, 3.78, and 5.63 J/m^2, and that the TiC a-plane is energetically most stable among these planes[32]. Therefore, it is considered that flat TiC domains with the c-plane are formed in the initial stage of the reaction

between Ti and HOPG by low-temperature annealing, although TiC domains agglomerate with a change to a pyramidal shape to preferably form a-plane facets by high-temperature annealing.

We also characterized the chemical reaction products after annealing the Ti/HOPG samples by ex situ XPS measurement. Figure 5 shows the photoelectron spectra of the Ti 2p core level obtained from the Ti (thickness: 0.25 nm)/HOPG samples as-deposited and after annealing at temperatures ranging from 600 to 1000 °C. In the case of the as-deposited sample, a Ti oxide component at binding energies of 464.5 and 458.8 eV for Ti $2p_{1/2}$ and Ti $2p_{3/2}$, respectively, is dominant[33]. In the spectrum for the as-deposited sample, the component related to the metal Ti, which was previously reported to have a binding energy of 453.8 eV for the Ti $2p_{3/2}$ core level[33], is hardly observed. This is considered to be due to the oxidation of a Ti metal layer during the sample transport in atmosphere from the deposition chamber to the ex situ XPS measurement system. This is because a Ti thin layer is a chemically active material and is easily oxidized even at RT.

On the other hand, the intensities of peaks at 460.7 and 454.7 eV for Ti $2p_{1/2}$ and Ti $2p_{3/2}$, respectively, significantly increase with annealing temperature, which can be considered to be the formation of TiC[34] through a chemical reaction between the Ti layer and HOPG takes place in high-temperature annealing. This result is consistent with the STM and RHEED observations mentioned above. Interestingly, note that we can identify the component related to TiC from the as-deposited Ti layer at RT on HOPG; although the intensity is lower than that of the annealed sample. This result suggests that TiC could be formed only by depositing Ti on graphite at RT. However, the component of TiC is limited in the as-grown sample, and we cannot determine in detail where the reaction preferentially occurs, for example, at the step in the HOPG surface. Considering the STM observation

mentioned above, we guess that the bonding structure at the interface between Ti and HOPG is dominated by Van der Waals force.

We summarize the crystalline structure and reaction between Ti and HOPG in Fig. 6. In the as-deposited Ti sample, the deposited Ti forms domains and epitaxially grows on HOPG, despite the fact than the bonding between Ti and HOPG by Van der Waals epitaxy is very weak [Fig. 6(a)]. After annealing at a low temperature in the range of 600–700 °C, the formation of epitaxial TiC domains through the reaction between Ti and HOPG takes place, and the surface of TiC becomes uniform and flat [Fig. 6(b)]. With the annealing temperature increased to 900 °C, TiC domains agglomerate with the formation of {111} facets [Fig. 6(c)], and the surface roughening of HOPG becomes significant especially around TiC domains after annealing at temperatures as high as 1000 °C [Fig. 6(d)].

4. Conclusions

We investigated the atomically crystalline structure of a Ti thin layer deposited on HOPG by in situ RHEED, STM, and ex situ XPS. We observed the epitaxial growth of Ti immediately after its deposition on HOPG at RT. After annealing above 600 °C, the formation of TiC proceeds with increasing annealing temperature, and STM and RHEED observations revealed the epitaxial growth of TiC with characteristic domains. The roughening of the surface of not only TiC but also HOPG substrates for annealing at temperatures as high as 900 °C. Considering these results, we have to control the atomic-scale interfacial reaction between the metal electrode and the low-dimensional graphite structure to form low-resistance contacts with high reliability for C nanoelectronics.

References

[1] S. Frank, P. Poncharal, Z. L. Wang, and W. A. de Heer, Science **280**, 1744 (1998).

[2] M. Shim, A. Javey, N. W. S. Kam, and H. Dai, J. Am. Chem. Soc. **123**, 11512 (2001).

[3] T. Dürkop, S. A. Getty , E. Cobas, and M. S. Fuhrer, Nano Lett. **4**, 35(2004).

[4] S. V. Morozov, K. S. Novoselov, F. Schedin, D. Jiang, A. A. Firsov, and A. K. Geim, Phys. Rev. B **72**, 201401(2005).

[5] K. Geim and K. S. Novoselov, Nat. Mater. **6**, 183 (2007).

[6] S. J. Kang, C. Kocabas, T. Ozel, M. Shim, N. Pimparkar, M. A. Alam, S. V. Rotkin, and J. A. Rogers, Nat. Nanotechnol. **2**, 230 (2007).

[7] F. Schwierz, Nat. Nanotechnol. 5, 487 (2010).

[8] E. J. H. Lee, K. Balasubramanian, R. T. Weitz, M. Burghard, and K. Kern, Nat. Nanotechnol. **3**, 486, (2008).

[9] P. Blake, R. Yang, S. V. Morozov, F. Schedin, L. A. Ponomarenko, A. A. Zhukov, R. R. Nair, I. V. Grigorieva, K. S. Novoselov, and A. K. Geim, Solid State Commun. **149**, 1068 (2009).

[10] S. Russo, M. F. Craciun, M. Yamamoto, A. F. Morpurgo, and S. Tarucha, Physica E **42**, 677 (2010).

[11] K. Nagashio, T. Nishimura, K. Kita, and A. Toriumi, Appl. Phys. Lett. **97**, 143514 (2010).

[12] Y. Matsuda, W.-Q. Deng, and W. A. Goddard III, J. Phys. Chem. C **114**, 17845 (2010).

[13] F. Xia, V. Perebeinos, Y.-M. Lin, Y. Wu and P. Avouris, Nat. Nanotechnol. **6**, 179 (2011).

[14] P. B. Abel, A. L. Korenyi-Both, F. S. Honecy, and S. V. Pepper J. Mater. Res. 9, 617 (1994).

[15] P. Marcus and C. Hinnen, Surf. Sci. **392**, 134 (1997).

[16] M. F. De Riccardis, D. Carbone, V. Martina, M. Re, B. Bozzini, and L. D'Urzo, Appl. Surf. Sci. 255, 4309 (2009).

[17] D.-Q. Yang, G.-X. Zhang, and E. Sacher, M. José-Yacamán, and N. Elizondo, J. Phys. Chem. B **110**, 8348 (2006).

[18] M.-H. Schaffnery, J.-F. Jeanneret, F. Patthey, and W.-D. Schneider, J. Phys. D **31**, 3177 (1998).

[19] H. Zhang, Q. Fu, Y. Yao, Z. Zhang, T. Ma, D. Tan, and X. Bao, Langmuir **24**, 10874 (2008).

[20] S. W. Poon, J. S. Pan, and E. S. Tok, Phys. Chem. Chem. Phys. **8**, 3326 (2006).

[21] E. Ganz, K. Sattler, and J. Clarkes, Surf. Sci. **219**, 33 (1989).
[22] V. Maurice and P. Marcus, Surf. Sci. **275**, 65 (1992).
[23] T. Endo, T. Sunada, T. Sumomogi, and H. Maeta, Mater. Charact. **48**, 159 (2002).
[24] I. Lopez-Salido, D. C. Lim, and Y. D. Kim, Surf. Sci. **588**, 6 (2005).
[25] I. Lopez-Salido, D. C. Lim, R. Dietsche, N. Bertram, and Y. D. Kim, J. Phys. Chem. B **110**, 1128 (2006).
[26] Inorganic Material Database (AtomWork) [http://crystdb.nims.go.jp/].
[27] A. Koma, K. Sunouchi, and T. Miyajima, Microelectron. Eng. **2**, 129 (1984).
[28] A. Koma, Thin Solid Films **216**, 72 (1992).
[29] K. Ueno, K. Sasaki, N. Takeda, K. Saiki, and A. Koma, Appl. Phys. Lett. **70**, 1104 (1997).
[30] M. Maret, B. Gilles, J.P. Simon, M. Verdier, I. Guhr, B. Riedlinger, M. Albrecht, and G. Schatz, J. Cryst. Growth **275**, 2289 (2005).
[31] H. Ito, H. Ichinose, C. Oshima, and T. Ichinokawa, Surf. Sci. Lett. **254**, L437 (1991).
[32] S. V. Dudiy and B. I. Lundqvist, Phys. Rev. B **69**, 125421 (2004).
[33] L. Ramqvist, K. Hamrin, G. Johansson, A. Fahlman, and C. Nordling, J. Phys. Chem. Solids **30**, 1835 (1969).
[34] H. Ihara, Y. Kumashiro, A. Itoh, and K. Maeda, Jpn. J. Appl. Phys. **12**, 1462 (1973).

Figure Captions

Fig. 1. (Color online) The STM images of the (a) Ti (thickness: 0.05 nm)/HOPG sample and (b) magnified one, and (c) Ti (thickness: 0.25 nm)/HOPG sample and (d) magnified one.

Fig. 2. In situ RHEED pattern of the Ti (thickness: 0.05 nm)/HOPG sample immediately after Ti deposition.

Fig. 3. (Color online) STM images of Ti (thickness: 0.25 nm)/HOPG samples after in situ annealing at (a) 700, (b) 900, and (c) 1000 °C.

Fig. 4. RHEED patterns of Ti (thickness: 0.25 nm)/HOPG samples after in situ annealing at (a) 700, (b) 900, and (c) 1000 °C.

Fig. 5. (Color online) Photoelectron spectra of the Ti 2p core-level obtained from Ti (thickness: 0.25 nm)/HOPG samples as-deposited and after annealing at 600, 700, 800, 900, and 1000 °C.

Fig. 6. (Color online) Schematic diagrams of crystalline structure and reaction between Ti and HOPG observed in this study. (a) As-deposited, and after annealing at (b) 600–700, (c) 900, and (d) 1000 °C.

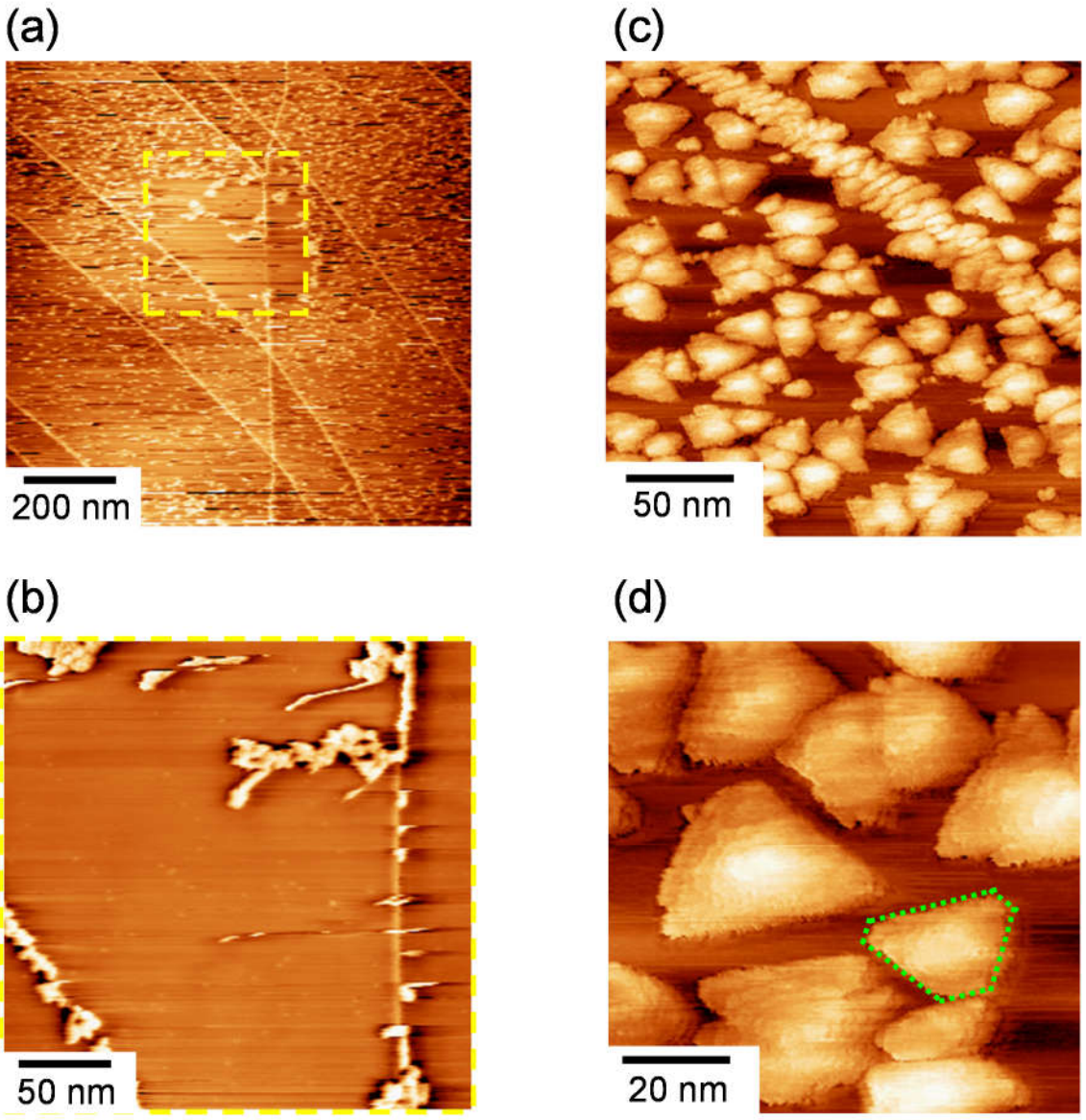

Fig. 1

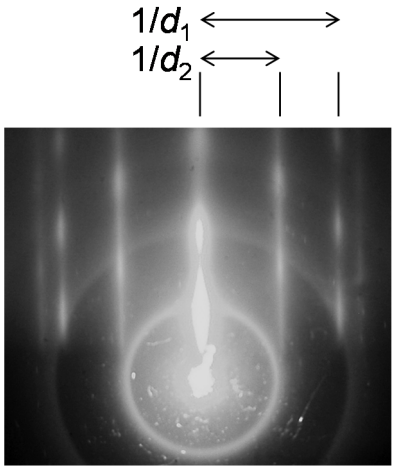

Fig. 2

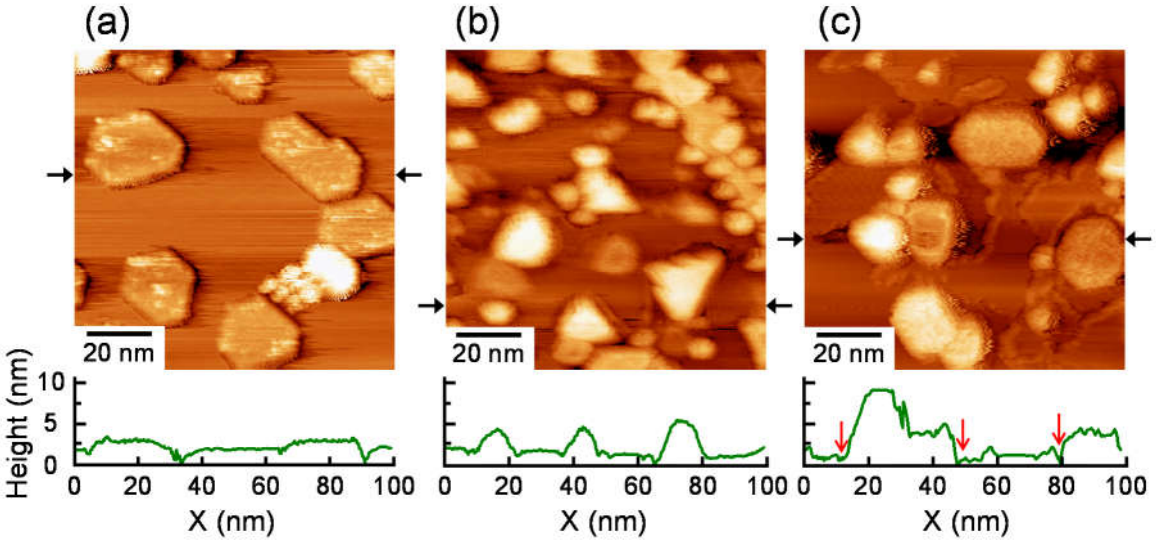
(a)
(b)
(c)
20 nm
20 nm
20 nm
Height (nm)
10
5
0
0 20 40 60 80 100
X (nm)
0 20 40 60 80 100
X (nm)
0 20 40 60 80 100
X (nm)

Fig. 3

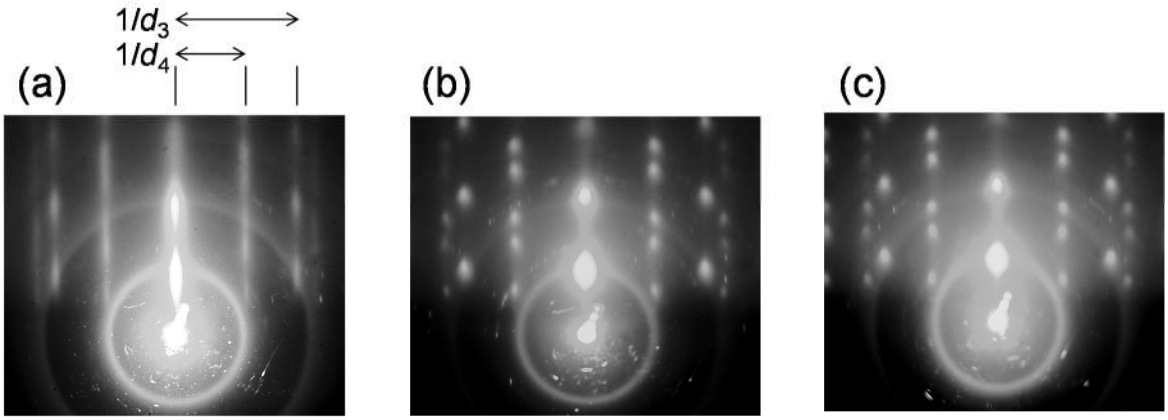

Fig. 4

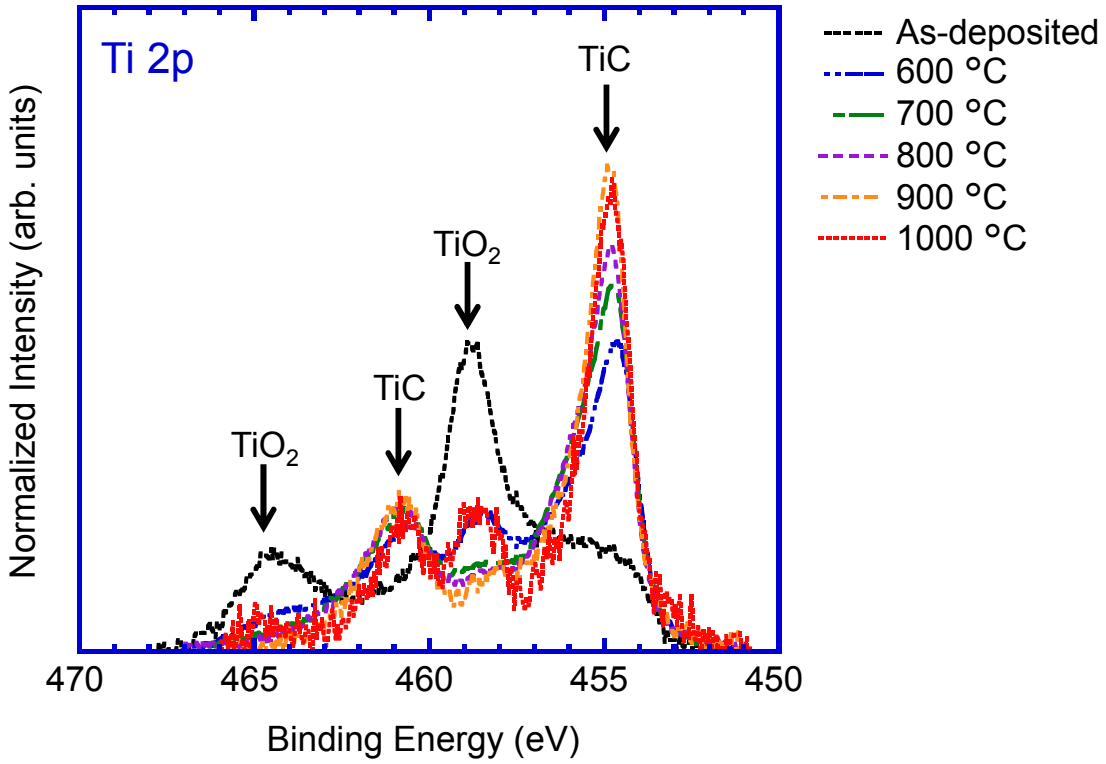
Ti 2p
TiC
TiO2
TiC
TiO2
As-deposited
600 °C
700 °C
800 °C
900 °C
1000 °C
Normalized Intensity (arb. units)
470
465
460
455
450
Binding Energy (eV)

Fig. 5

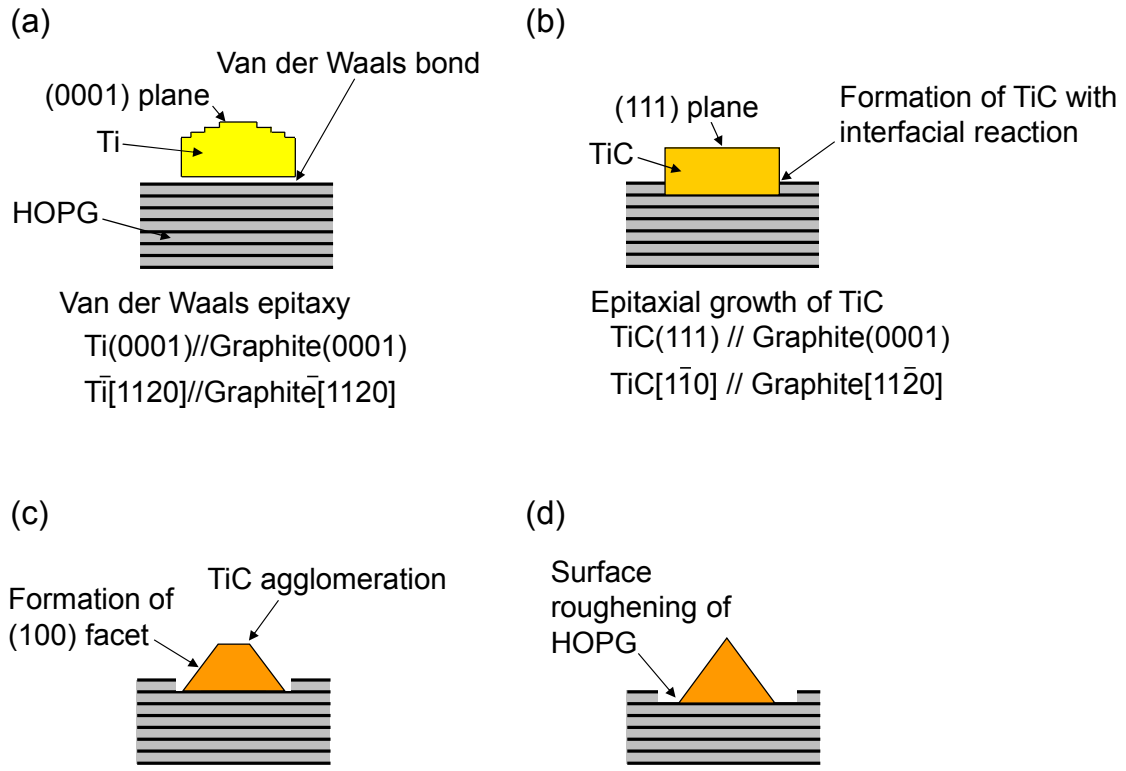
(a)
Van der Waals bond
(0001) plane
Ti
HOPG
Van der Waals epitaxy
Ti(0001)//Graphite(0001)
Ti[1120]//Graphite[1120]
(b)
(111) plane
Formation of TiC with interfacial reaction
TiC
Epitaxial growth of TiC
TiC(111) // Graphite(0001)
TiC[1$\bar{1}$0] // Graphite[11$\bar{2}$0]
(c)
TiC agglomeration
Formation of (100) facet
(d)
Surface roughening of HOPG

Fig. 6